Bone marrow-derived fibroblast precursors mediate ischemic cardiomyopathy in mice

Sandra B. Haudek*, Ying Xia*, Peter Huebener*, John M. Lee*, Signe Carlson*, Jeff R. Crawford†, Darrell Pilling†, Richard H. Gomer†, JoAnn Trial*, Nikolaos G. Frangogiannis*, and Mark L. Entman*‡

*DeBakey Heart Center, Baylor College of Medicine and Methodist Hospital, Houston, TX 77030; and †Howard Hughes Medical Institute, Department of Biochemistry and Cell Biology, Rice University, Houston, TX 77005

Communicated by Lutz Birnbaumer, National Institutes of Health, Research Triangle Park, NC, October 4, 2006 (received for review August 31, 2006)

We previously described a mouse model of fibrotic ischemia/reperfusion cardiomyopathy (I/RC) arising from daily, brief coronary occlusion. One characteristic of I/RC was the prolonged elevation of monocyte chemoattractant protein 1 (MCP-1), which was obligate to its phenotype and may contribute to the uptake of bloodborne cells. Here we describe in I/RC hearts a population of small spindle-shaped fibroblasts that were highly proliferative and expressed collagen I and α-smooth muscle actin (myofibroblast markers), CD34 (a precursor marker), and CD45 (a hematopoietic marker). These cells represented 3% of all nonmyocyte live cells. To confirm the cells' bone marrow origin, chimeric mice were created by the rescue of irradiated C57BL/6 mice with marrow from ROSA26, a congenic line expressing lacZ. I/RC resulted in a large population of spindle-shaped fibroblasts containing lacZ. We postulated that the fibroblast precursors represented a developmental path for a subset of monocytes, whose phenotype we have shown to be influenced by serum amyloid P (SAP). Thus, we administered SAP *in vivo*, which markedly reduced the number of proliferative spindle-shaped fibroblasts and completely prevented I/RC-induced fibrosis and global ventricular dysfunction. By contrast, SAP did not suppress the inflammation or chemokine expression seen in I/RC. SAP, a member of the pentraxin family, binds to Fcγ receptors and modifies the pathophysiological function of monocytes. Our data suggest that SAP interferes with assumption of a fibroblast phenotype in a subset of monocytes and that SAP may be an important regulator in the linkage between inflammation and nonadaptive fibrosis in the heart.

fibrosis | heart | monocyte chemoattractant protein 1 | monocytes | serum amyloid P

Deposition and remodeling of connective tissue in the heart plays a critical role in cardiac repair and response to injury. Although fibrosis is critical to wound healing and tissue repair, it is also clearly an important pathogenic feature of many myocardial diseases (1). Accumulation of collagen occurs as a "replacement" mechanism in response to cardiac myocyte necrosis, which leads to repair and scar formation (2). However, fibrosis also occurs on a reactive basis around coronary vessels (perivascular fibrosis) and in the interstitial space (2, 3). It is generally considered that both reactive and reparative fibrosis may contribute to adverse remodeling. In the fibrotic heart, collagen accumulation may lead to cardiac dysfunction and muscle fiber entrapment (2), increased myocyte loss (4), and myocyte atrophy (5), as well as electrical anisotropy and reentrant arrhythmias (6, 7). However, despite its recognized role in the pathology of cardiovascular disease, the mechanism(s) responsible for the development of fibrosis are not well understood.

In our previous work, we developed a murine model of closed-chest myocardial infarction and reperfusion that allowed examination of chemokine induction after dissipation of surgical trauma (8). We found that 15 min of ischemia induced reactive oxygen-dependent chemokine expression in the absence of infarction (9). We then examined the consequences of multiple, daily 15-min occlusions in the mouse heart, which was not attended by cardiomyocyte necrosis (10, 11). In contrast to infarction, this protocol resulted in a fibrotic cardiomyopathy accompanied by global ventricular dysfunction (ischemia/reperfusion cardiomyopathy; I/RC). I/RC was associated with markedly prolonged induction of the potent mononuclear cell chemokine monocyte chemoattractant protein 1 (MCP-1); the mRNA peaked at 3 d and remained significantly elevated for >1 week (10). The pathology of I/RC largely resembled that which we described in samples from patients with "hibernating myocardium" (12, 13). The data suggested that daily episodes of I/RC resulted in the production of reactive oxygen and subsequent prolonged induction of MCP-1 (10). The cardiac dysfunction could be prevented by overexpression of extracellular superoxide dismutase (10) and by either genetic deletion of MCP-1 or injection of a neutralizing anti-MCP-1 antibody (14).

In the study described here, we pursued the hypothesis that prolonged induction of the mononuclear chemokine MCP-1 resulted in uptake of bloodborne cells critical to the pathophysiology of I/RC. The data suggest that, in addition to the uptake of monocytes, I/RC was associated with the uptake of a bone marrow-derived, bloodborne population of fibroblast precursors of hematologic origin. These precursors gave rise to a population of small spindle-shaped fibroblasts that were highly proliferative and were not present in sham or control animals. These fibroblasts expressed collagen I and α-smooth muscle actin (α-SMA) characteristic of myofibroblasts and also expressed CD34, a marker of precursor cells, and CD45, the canonical marker for hematopoietic cells. We discuss their origin as a developmental path for a subset of blood monocytes.

Data from the literature describe a subpopulation of mononuclear cells ("fibrocytes") that, when cultured in the absence of serum, assume a phenotype of spindle-shaped morphology with expression of CD34 and fibroblast antigens (15–17). Our recent work demonstrated that the assumption of the fibrocyte phenotype among cells in the mononuclear cell population was markedly inhibited by the pentraxin serum amyloid P (SAP) (17). Thus, we treated mice with daily injections of SAP while they were undergoing the I/RC protocol. Treated animals did not develop either the fibrosis or the cardiac dysfunction associated with the I/RC protocol. Moreover, the presence of $CD34^+$/$CD45^+$ spindle-shaped fibroblasts was largely eliminated. Thus,

Author contributions: S.B.H., D.P., R.H.G., J.T., N.G.F., and M.L.E. designed research; S.B.H., Y.X., P.H., J.M.L., and S.C. performed research; J.R.C., D.P., and R.H.G. contributed new reagents/analytic tools; S.B.H., P.H., J.T., and M.L.E. analyzed data; and S.B.H., J.T., and M.L.E. wrote the paper.

Conflict of interest statement: Rice University has patent applications on the use of SAP to inhibit fibrosis, and this intellectual property has been licensed to Medior Biopharm. D.P. and R.H.G. are founding members of, have equity in, and receive royalties from Medior Biopharm.

Freely available online through the PNAS open access option.

Abbreviations: α-SMA, α smooth muscle actin; FcγR, Fcγ receptor; I/RC, ischemia/reperfusion cardiomyopathy; MCP-1, monocyte chemoattractant protein 1; SAP, serum amyloid P.

‡To whom correspondence should be addressed at: DeBakey Heart Center, 6565 Fannin Street, M/S F-602, Houston, TX 77030. E-mail: mentman@bcm.tmc.edu.

www.pnas.org/cgi/doi/10.1073/pnas.0608799103

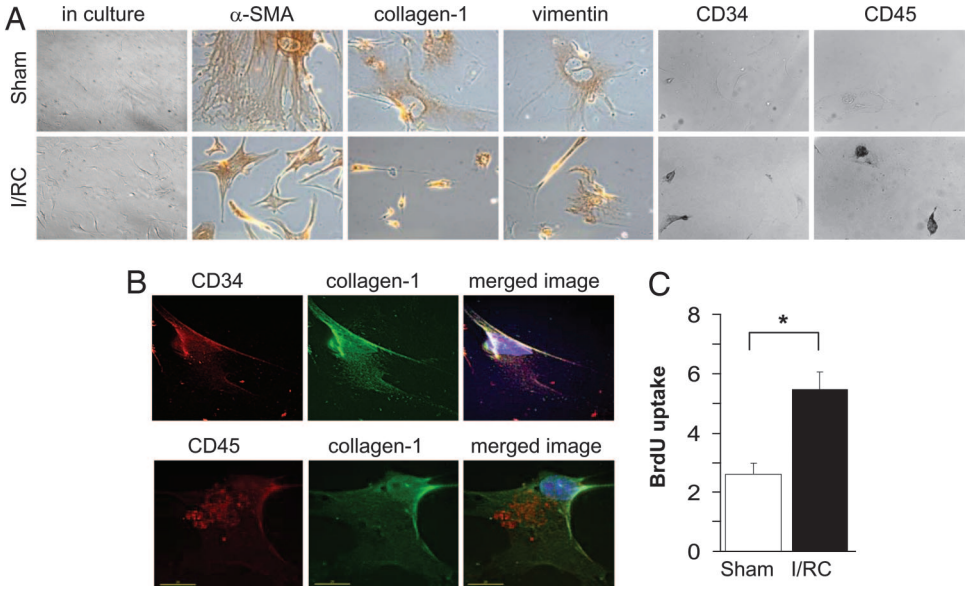

Fig. 1. Characterization of cardiac fibroblasts after 5-d I/RC. (*A*) Isolated fibroblasts cultured *in vitro* (panel 1, magnification: ×100) were tested for the presence/absence of cell markers by immunocytochemistry (panels 2–6, magnification: ×200). (*B*) Freshly isolated $CD34^+$ or $CD45^+$ cells (red) were sorted by immunoabsorption, plated on coverslips, and stained for collagen I (green; blue indicates DAPI-stained nuclei). (*C*) Proliferation of cardiac fibroblasts *in vitro* was determined by BrdU incorporation. Values represent the fold induction of growth rate induced by 10% serum compared with serum-free medium (*, $P < 0.01$; $n = 6$ per group).

our data suggest an important role for bone marrow-derived, bloodborne fibroblast precursors of hematologic origin that are critical to the development of I/RC. The data also suggest that pentraxins, which are ligands for the Fcγ receptors (FcγR) on leukocytes, may regulate phenotypic transition of cells within the monocyte fraction. The possibility that this autacoidal interaction through FcγR represents a mechanism of cross-talk between inflammatory and fibrotic reactions in the pathophysiology of nonadaptive fibrosis in the heart is considered.

Results

Cardiac Fibroblasts. After 5-d I/RC, virtually all isolated cardiac fibroblasts cultured *in vitro* expressed α-SMA, collagen I, and vimentin (Fig. 1*A*) but not myosin, desmin, or CD31 (data not shown). Fibroblasts from sham animals were large and flat with long processes, whereas fibroblasts from I/RC animals consisted mainly of smaller, spindle-shaped cells. Many of the small spindle-shaped cells were $CD34^+$ and $CD45^+$, whereas large flat cells were not, indicating that after I/RC a subpopulation of cardiac fibroblasts was of hematopoietic precursor origin. No $CD34^+$ or $CD45^+$ cells were found in fibroblast isolations from sham animals (Fig. 1*A*). $CD34^+$ and $CD45^+$ cells were also positive for collagen I, a distinctive fibroblast marker (Fig. 1*B*). In addition, cardiac fibroblasts from I/RC animals proliferated twice as fast as fibroblasts from sham animals (Fig. 1*C*).

Immunohistochemical examination of tissue from I/RC animals confirmed the presence of $CD45^+$ myofibroblasts expressing α-SMA^+ (Fig. 2*A*). By using flow cytometry, we found that freshly dispersed nonmyocyte cardiac cells after I/RC contained (mean ± SEM) 5.1 ± 0.8% $CD34^+$ and 9.8 ± 1.2% $CD45^+$ cells, with 3.1 ± 0.5% being positive for both markers (Fig. 2*B*). In particular, as seen in a representative cytometric diagram, 60% of all $CD34^+$ cells were also positive for CD45, and 30% of all $CD45^+$ cells were positive for CD34 (Fig. 2*C*). Further, 73 ± 9% of all $CD34^+$ cells were collagen I^+, whereas 7 ± 3% of all collagen I^+ cells were $CD34^+$. Similarly, 41 ± 4% of all $CD45^+$ cells were collagen I^+, whereas 13 ± 1% of all collagen I^+ cells were $CD45^+$ (see also Fig. 6, which is published as supporting information on the PNAS web site). We also found that ≈50% of the $CD34^+$ and $CD45^+$cells also expressed the canonical cardiac fibroblast marker discoidin domain receptor 2.

Chimeric Mouse Model. To confirm a bone marrow-derived fibroblast precursor origin, we subjected chimeric mice [C57BL/6 mice with substitute bone marrow from ROSA26 ($lacZ^+$)] to 5-d I/RC. Isolated cardiac fibroblasts from untreated chimeric mice cultured *in vitro* were negative for lacZ expression as tested by X-gal staining. After I/RC, however, the majority of small spindle-shaped cells stained positive for lacZ, whereas large flat cells did not (Fig. 3*A*). Moreover, small spindle-shaped β-galactosidase$^+$ cells were positive for α-SMA, collagen I, and CD34 (Fig. 3 *B* and *C*), whereas large flat β-galactosidase$^-$ cells were positive for α-SMA and collagen I but negative for CD34 (Fig. 3 *B* and *C*).

Effect of SAP. To examine whether the effect of SAP on the *in vitro* fibrocyte reaction (17) was pertinent *in vivo*, we tested whether SAP also interferes with assumption of the fibroblast phenotype from bloodborne precursors in I/RC. After 5-d I/RC with SAP treatment, isolated cardiac fibroblasts cultured *in vitro* consisted almost entirely of large flat cells, and the number of small spindle-shaped cells was negligible (Fig. 4*A*). The cells from SAP-treated hearts also proliferated more slowly than fibroblasts after I/RC without SAP treatment (Fig. 4*B*) and were not noticeably different from fibroblasts isolated from sham animals (compare with Fig. 1*C*).

Freshly dispersed nonmyocyte cardiac cells after I/RC with SAP treatment contained significantly fewer $CD34^+$ cells (1.2 ± 0.5%; Fig. 4*C*) than after I/RC without treatment. Similarly, the number of cells positive for both CD34 and CD45 was significantly reduced by SAP treatment (0.7 ± 0.3%; Fig. 4*C*). By contrast, although modestly reduced, the presence of $CD45^+$ cells was not significantly changed by SAP treatment (6.6 ± 0.8%; Fig. 4*C*). This finding correlated with the histologic observation that SAP treatment had no significant effect on macrophage number (237 ± 30 vs. 203 ± 31 cells per mm^2; Fig. 4*D*).

Staining of perfusion-fixed heart tissue also demonstrated that SAP treatment decreased the number of I/RC-induced α-SMA^+

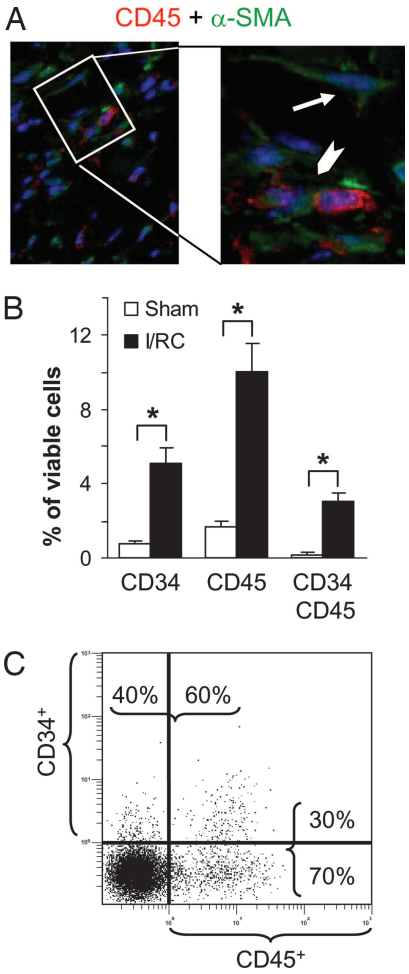

Fig. 2. CD34 and CD45 expression. (*A*) Perfusion-fixed heart tissue was stained for α-SMA (green) and CD45 (red) to identify myofibroblasts. The arrowhead indicates a cell positive for both markers, whereas the arrow indicates an α-SMA$^+$ smooth muscle cell in the wall of an adjacent venule. Also present are CD45$^+$ α-SMA$^-$ cells that represent infiltrating macrophages. (*B*) Cytometric analysis of freshly dispersed nonmyocyte cardiac cells for CD34 and CD45 expression of viable (calcein$^+$) cells in sham and I/RC animals (*, $P < 0.001$; $n = 8$ per sham and 10 per I/RC). (*C*) Representative cytometric diagram for three-color staining (*x* axis, PE/Cy-5-CD45; *y* axis, PE-CD34; gated on calcein$^+$ cells).

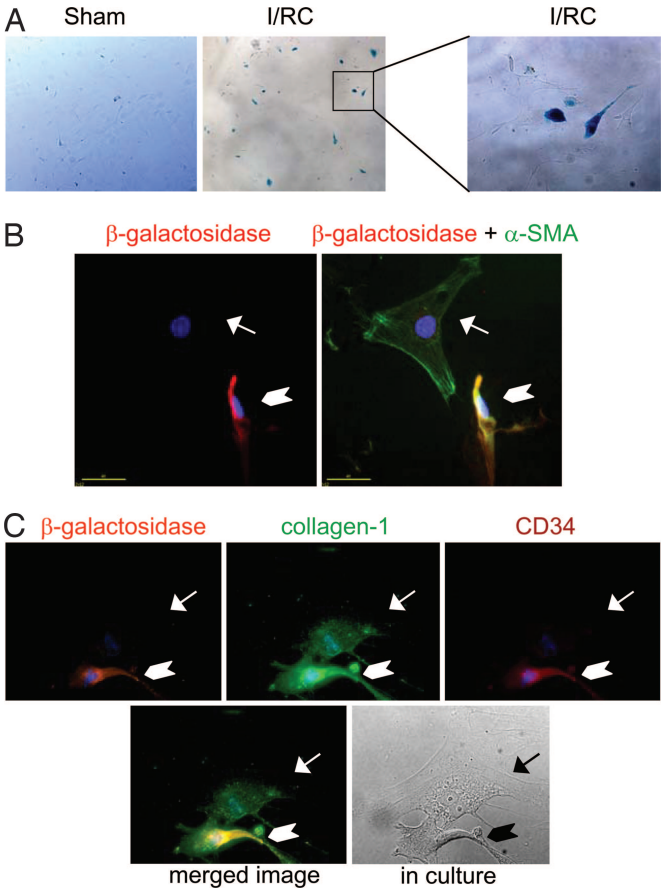

Fig. 3. Cardiac fibroblasts from chimeric mice (ROSA26 bone marrow donor cells to C57BL/6 recipient mice) after 5-d I/RC. (*A*) Cultured fibroblasts were stained with X-gal to visualize bone marrow-originating cells (lacZ$^+$ cells). (Magnification: *Left* and *Center*, ×100; *Right*, ×200.) After I/RC, many small spindle-shaped cells stained positive (blue) for lacZ expression, whereas no positive cells were found in sham animals. (*B* and *C*) Further immunocytochemistry analysis using a specific antibody against β-galactosidase demonstrated that only small spindle-shaped cells (arrowheads) but not large flat cells (arrows) were positive for lacZ (red), although both cell populations expressed the fibroblast markers α-SMA (green; *B*; scale bar, 40 μm) and collagen I (green; *C*). LacZ$^+$ cells also expressed CD34 (cyan; *C*), whereas large flat cells did not. Blue indicates DAPI-stained nuclei; yellow results from merging images.

cells (15.4 ± 6.0 vs. 2.4 ± 0.7 cells per mm^2; Fig. 4*E*). Similarly, SAP treatment reduced the amount of collagen deposition induced by I/RC when compared with untreated I/RC animals (4.9 ± 0.4% vs. 2.0 ± 0.2% area; Fig. 4*F*), indicating that SAP inhibited the development of fibrosis in this model.

As described previously (10), I/RC induced global ventricular dysfunction manifested by reduced fractional shortening and decreased anterior wall thickening. Administration of SAP significantly improved fractional shortening (34 ± 2% vs. 43 ± 2%; Fig. 5*A*) and preserved anterior wall thickening (36 ± 3% vs. 53 ± 3%; Fig. 5*B*), thus preventing I/RC-induced cardiac dysfunction. Values for fractional shortening and anterior wall thickening of SAP-treated I/RC animals were not different from sham values, demonstrating virtually complete protection of cardiac function associated with the cellular effects described in Figs. 3 and 4.

As reported earlier, I/RC induced mRNA expression of MCP-1 and osteopontin but not of other chemokines and/or cytokines (10). Administration of SAP to animals undergoing I/RC did not diminish this observed increase in MCP-1 mRNA expression, nor did SAP alter expression of other chemokines and/or cytokines tested (Fig. 5 *C* and *D*).

Discussion

The data reported here address the role of the immune system in nonadaptive fibrosis. Understanding the pathologic mechanisms responsible for nonadaptive fibrosis has been difficult due to the lack of reproducible animal models of ischemic heart disease in the absence of cardiomyocyte death and to the likelihood that fibrosis is multifactorial. Thus, we have developed I/RC, a murine closed-chest model of fibrotic cardiomyopathy, in which repetitive 15-min ischemia followed by 24-h reperfusion induces fibrosis and global ventricular dysfunction in the absence of myocardial infarct (10). The demonstration that SAP-inhibited fibrosis and cellular changes also obviated cardiac dysfunction in I/RC confirmed I/RC as a model of nonadaptive fibrosis.

A hallmark of the I/RC model is the chemokine up-regulation that leads to prolonged expression of MCP-1, a potent monocytic chemoattractant protein, suggesting the possible importance of

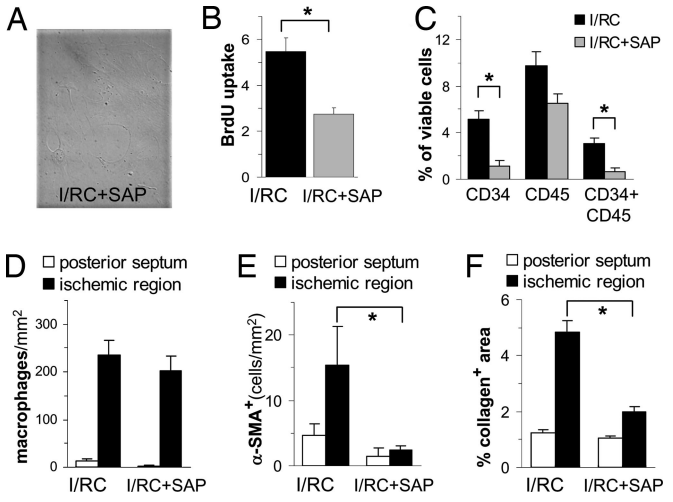

Fig. 4. Cellular effects of SAP. (*A*) Isolated cardiac fibroblasts after 5-d I/RC with SAP treatment cultured *in vitro* were large and flat, similar to sham fibroblasts (see Fig. 1*A*). (Magnification: ×100.) (*B*) Proliferation of these cells was determined by BrdU incorporation in response to 10% serum compared with serum-free medium. Note that fibroblasts after I/RC with SAP treatment proliferated significantly more slowly than fibroblasts without SAP and were not different from sham fibroblasts (see Fig. 1*C*) (*, $P < 0.02$; $n = 6$ per group). (*C*) Cytometric analysis of dispersed nonmyocyte cardiac cells for CD34 and CD45 expression of viable (calcein$^+$) cells in 5-d I/RC animals with and without SAP treatment. Note that SAP significantly reduced the number of CD34$^+$ cells (*, $P < 0.001$; $n = 10$ per group) and CD34$^+$/CD45$^+$ cells (*, $P < 0.003$; $n = 6$ per group) but not the number of CD45$^+$ cells ($P > 0.05$; $n = 10$ per group). (*D–F*) Quantitative analysis of macrophage (*D*) and myofibroblast density (*E*), as well as collagen content (*F*), in the ischemic myocardium was performed in perfusion-fixed hearts. The posterior septum region served as an internal control because this region should not be affected by I/RC. Note that SAP did not diminish macrophage infiltration ($P > 0.05$, $n = 5$ per group), indicating that I/RC-induced inflammation was not inhibited by SAP. However, treatment with SAP significantly reduced the number of myofibroblasts in tissue (*, $P < 0.05$; $n = 4$ per group) and blunted the development of fibrosis (*, $P < 0.001$; $n = 6$ per group) after I/RC.

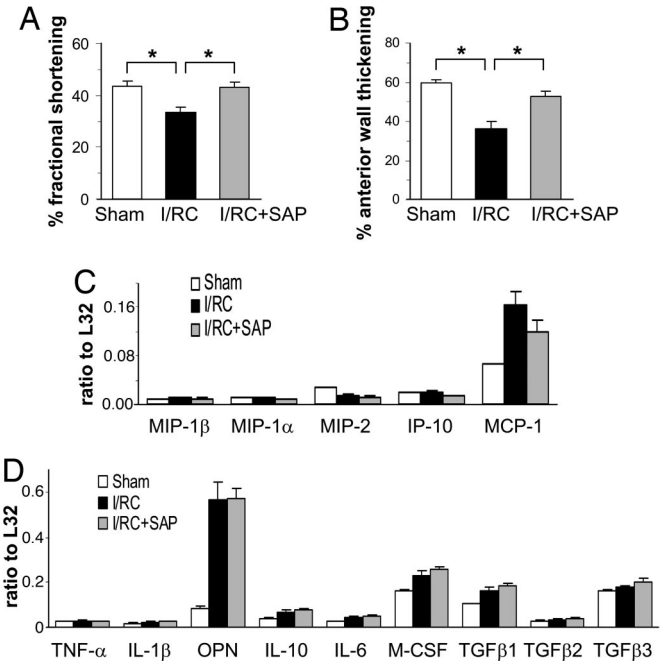

Fig. 5. Effects of SAP on ventricular function and mRNA expression. SAP treatment improved fractional shortening (*, $P < 0.05$; $n = 7$ per group) (*A*) and preserved anterior wall thickening (*, $P < 0.001$; $n = 7$ per group) (*B*) in mice undergoing I/RC as measured by M-mode echocardiography and were similar to results for sham-operated animals ($P > 0.05$, $n = 7–8$ per group). SAP treatment did not alter I/RC-induced mRNA expression of MCP-1 ($P = 0.15$; $n = 8$ per group) and/or other chemokines (*C*) or cytokines (*D*). (See section *RNA* in *Materials and Methods* for abbreviations.)

chemokinetically driven uptake of bone marrow-derived, blood-borne cells. In this article we now extend our studies, describing the obligate role of uptake of a CD34$^+$/CD45$^+$ fibroblast precursor population arising from the bone marrow in fibrosis and cardiac dysfunction in I/RC. We and others (18–22) have previously demonstrated that hematopoietic precursor cells migrate into the border zone of the myocardial infarction and differentiate into cardiac myocytes and endothelial cells. The literature provides further evidence for marrow-derived precursor uptake of smooth muscle cells, inflammatory cells, and mast cells into the injured heart (22–24). In addition, bone marrow-derived fibroblast progenitor cells have been shown to be critical in pulmonary fibrosis and wound healing (15, 16, 25, 26). The uptake of such cell precursors from the fibrocyte precursor population has also been demonstrated in skin and lung (26–28).

We here demonstrated that isolated cardiac fibroblasts after I/RC obtained a distinctive morphology of small spindle-shaped cells next to large flat cells. The vast majority of these spindle-shaped cells expressed not only fibroblast markers such as collagen I and α-SMA, but also the precursor marker CD34 and the hematopoietic maker CD45, indicating that these cells arise from a hematologic origin. We showed that this CD34$^+$/CD45$^+$ cell population made up 3% of all live non-cardiomyocyte cells, as measured by flow cytometry. This subset of cells represented ≈30% of all CD45$^+$ cells and ≈60% of all CD34$^+$ cells. The remaining CD45$^+$/CD34$^-$ cell population might constitute inflammatory cells that were present in the myocardium after I/RC. Inflammation in I/RC was profound and has been characterized extensively in previous reports from our laboratory (10, 11). Similarly, the remaining CD34$^+$/CD45$^-$ cell population might represent endothelial precursor cells, as described by Dimmeler and coworkers (21).

To confirm the hematopoietic origin of fibroblast precursors, we used chimeric mice that expressed β-galactosidase in bone marrow-originating cells. We showed that after I/RC a subpopulation of isolated cardiac fibroblasts was positive for lacZ expression, as well as for CD34 and collagen I. The phenotype of these cells closely resembled that of a mononuclear cell population termed "fibrocytes" (15, 16) that arise after culturing blood cells *in vitro* without serum, with the exception that the cardiac fibroblast subpopulation proliferated rapidly, whereas fibrocytes did not proliferate in culture (17). Recently, we have shown that SAP, a serum factor closely related to C-reactive protein, prevented the appearance of fibrocytes in cultured peripheral blood monocytes (17). SAP is a member of the pentraxin family of autacoids that bind to FcγR and modify the phenotype and pathophysiological function of monocytes (29, 30). We therefore elected to use SAP in our fibrotic cardiomyopathy model to determine whether inhibition of circulating monocyte differentiation resulted in reduced fibrosis after I/RC. Indeed, our results indicated that administration of SAP during I/RC not only prevented non-adaptive fibrosis in the heart but also improved global and regional ventricular dysfunction as measured by greater fractional shortening and preserved anterior wall thickening. In addition, after SAP treatment, isolated fibroblasts lacked the small spindle-shaped morphology and were not different from isolated fibroblasts from sham hearts. Most importantly, after SAP treatment we could not detect the CD34$^+$/CD45$^+$ subpopulation of fibroblasts characteristic of I/RC.

Our previous studies (14) suggested an obligate role for prolonged MCP-1 expression in I/RC and the attendant fibrotic inflammation and cardiac dysfunction. As a result, we propose that the $CD45^+$ fibroblast precursors arose from a subset of the mononuclear cell fraction. SAP did not affect the induction of MCP-1 or other chemokines and cytokines. Similarly, SAP did not reduce macrophage content in I/RC. This finding indicates that uptake of a precursor from the mononuclear population was not reduced. Thus, we hypothesize that SAP more likely inhibited the maturation of precursors to fibroblasts in a manner similar to that seen in the *in vitro* fibrocyte assay. In the latter, we have shown that fibrocyte formation was inhibited by SAP (17) but also by macroaggregated IgG binding to FcγR (31). Signaling through FcγR is well known to exert potent effects on monocyte phenotypes (32); it is tempting to suggest a regulatory role for FcγR in the maturation of fibroblasts from the population of monocytes taken up in an inflammatory reaction. If this role is operative, it would suggest a link between inflammation and immunological actors in nonadaptive fibrosis.

Conclusion

Nonadaptive fibrosis in a model of ischemic cardiomyopathy is associated with an MCP-1-driven uptake of bone marrow-derived, bloodborne fibroblast precursor(s) of hematopoietic origin, as well as monocytes. The pentraxin SAP markedly reduced the presence of $CD34^+/CD45^+$ fibroblasts and fibrosis and totally inhibited cardiac dysfunction in this model; SAP did not alter leukocyte uptake or chemokine or cytokine levels. We suggest that SAP, a ligand for FcγR, influences the phenotype of the monocytic population and inhibits maturation of a fibroblast precursor. This role for SAP is a potential link of nonadaptive fibrosis to inflammation and immunologic factors.

Materials and Methods

For more detail regarding the following procedures, see *Supporting Materials and Methods*, which is published as supporting information on the PNAS web site.

I/RC. C57BL/6 mice were subjected to closed-chest surgery as described previously (8, 10). The time points for maximal chemokine mRNA expression (3 d), fibroblast activation (5 d), and fibrosis and cardiac dysfunction (7 d) were determined previously (10). All animals were used in accordance with the guidelines of the Baylor College of Medicine Animal Care and Research Advisory Committee and with the rules governing animal use as published by the National Institutes of Health.

Chimeric Mice. Bone marrow cells (1×10^6) from ROSA26 mice were transferred to irradiated C57BL/6 mice, as described previously (18, 19). Six to 8 weeks after transplantation, animals with >60% engraftment were used for experiments.

SAP. SAP was purified from mouse serum (Sigma-Aldrich, St. Louis, MO) as described earlier (33). Thirty minutes before daily occlusion, mice received 50 μg of mouse SAP i.p. (I/RC+SAP group) or the equivalent molar dose (25 μg) of mouse albumin (Sigma-Aldrich) (I/RC group).

Cell Isolation. Cardiac fibroblasts were isolated by using 0.25 mg/ml Liberase Blendzyme 4 (Roche Applied Science, Indianapolis, IN). Cells were immediately used for experiments or were cultured in DMEM/F-12 (GibcoBRL/Invitrogen, Carlsbad, CA)/10% FBS (HyClone, Logan, UT).

Flow Cytometry. Cells (1×10^5) were incubated with 50 nM calcein (Molecular Probes, Carlsbad, CA) and 0.5 μg of PE-anti-CD34, biotin-anti-CD45/avidin-PE/Cy-5 (all from BD PharMingen, San Diego, CA), anti-discoidin domain receptor 2 (a gracious gift from Thomas Borg, University of South Carolina, Columbia, SC), or anti-collagen I (Rockland, Gilbertsville, PA). If necessary, cells were permeabilized by using the Cytofix/Cytoperm kit (BD PharMingen) in accordance with the manufacturer's protocol. FITC/PE/Cy-5 fluorescence intensities were measured on a Beckman Coulter (Fullerton, CA) Epics XL-MCL flow cytometer using EXPO32 software.

Immunoabsorption. Cells (2×10^6) were incubated with 1 μg of PE-anti-CD34 or PE-anti-CD45 before being put onto anti-PE coated bacteriological plates. Nonadherent cells were carefully washed off, and adherent $CD34^+$ or $CD45^+$ cells were removed by subsequent vigorous washing.

Proliferation. Proliferation was determined by BrdU incorporation using a colorimetric kit from Roche Applied Science as described by the manufacturers. Emission was measured on a standard ELISA plate reader (Spectra Max 250; Molecular Devices, Sunnyvale, CA). Enhanced proliferation in response to 10% serum was expressed as fold increase to cells maintained in serum-free medium.

Immunocytochemistry. Cells (1×10^4) were cultured on poly-L-lysine coverslips (BD BioCoat, San Diego, CA), fixed in Histochoice (Amresco, Solon, OH), permeabilized with 0.1% Triton X-100, and incubated in primary antibody followed by biotin-conjugated secondary antibody. Staining was visualized either by HRP on a microscope equipped with a digital camera (AxioCam HRc; Carl Zeiss MicroImaging, Thornwood, NY) or by fluorescence (Delta Vision Spectris; Applied Precision, Issaquah, WA; images were digitally photographed and analyzed using softWoRx). The following antibodies were used: vimentin, α-SMA, smooth muscle myosin, and desmin (all from Sigma-Aldrich), Pecam-1 (BD PharMingen), and β-galactosidase (Chemicon, Temecula, CA). Detection of β-galactosidase was also performed using X-gal (Roche Applied Science).

Histology. Tissue sections were prepared as described previously (12). Collagen deposition was determined by staining with picrosirius red (Poly Scientific, Bay Shore, NY). The collagen-stained area in the ischemic anterior wall and in the nonischemic posterior septum (control) was calculated as a percentage of the total myocardial area. Myofibroblast density was determined by counting the number of interstitial α-SMA^+ cells, and macrophage density by counting the number of Mac-2^+ (Cedarlane, Burlington, NC) cells. For detection of $CD45^+/\alpha$-SMA^+ cells in tissue, deparaffinized heart sections were autoclaved in 10 mM citrate buffer, pH 6.0/0.05% Tween 20 at 121°C for 4 min before antibody incubation. To quench autofluorescence, sections were exposed to cold 0.3% Sudan Black in 70% ethanol.

Echocardiography. Echocardiography was performed before the first ischemic episode and 5 h after the last ischemic episode, as described previously (10).

RNA. Levels of chemokine [macrophage inflammatory protein (MIP)-1β, -1α, and -2; IFN-γ-induced protein (IP)-10; and MCP-1] and cytokine [TNF-α; IL-1β, -6, and -10; osteopontin (OPN); macrophage colony-stimulating factor (M-CSF); and TGF-β1, -β2, and -β3] mRNA expression were determined by ribonuclease protection assay (RiboQuant; BD PharMingen) as described previously (10).

Statistical Analysis. All data are expressed as mean ± SEM. Two-tailed, unpaired Student's *t* test was used to determine a significant difference between two groups. One-way ANOVA was used to evaluate differences between three or more groups.

Post hoc testing (Tukey–Kramer method) was performed when appropriate. $P < 0.05$ was considered statistically significant.

We thank Thuy Pham, Stephanie Butcher, and Claudia Aguillon for expert technical assistance and Dr. Margaret Goodell for advice and assistance in the generation of chimeric mice. This work was supported by National Heart, Lung, and Blood Institute Grants HL-42550 and R01 HL-076661, The Medallion Foundation, and The Methodist Hospital Foundation (to S.B.H., J.T., and M.L.E.); by National Heart, Lung, and Blood Institute Grant R01 HL-76246 (to N.F.G.); and by The Howard Hughes Medical Institute and The Robert A. Welch Foundation Grant C-1555 (to D.P. and R.H.G.).

1. Brilla CG, Weber KT (1992) *Cardiovasc Res* 26:671–677.
2. Weber KT, Brilla CG, Janicki JS (1993) *Cardiovasc Res* 27:341–348.
3. Weber KT, Pick R, Jalil JE, Janicki JS, Carroll EP (1989) *J Mol Cell Cardiol* 21(Suppl 5):121–131.
4. Weber KT, Janicki JS, Pick R, Capasso J, Anversa P (1990) *Am J Cardiol* 65:1G–7G.
5. Jalil JE, Janicki JS, Pick R, Abrahams C, Weber KT (1989) *Circ Res* 65:258–264.
6. Thiedemann KU, Holubarsch C, Medugorac I, Jacob R (1983) *Basic Res Cardiol* 78:140–155.
7. Bing OH, Matsushita S, Fanburg BL, Levine HJ (1971) *Circ Res* 28:234–245.
8. Frangogiannis NG, Smith CW, Entman ML (2002) *Cardiovasc Res* 53:31–47.
9. Nossuli TO, Frangogiannis NG, Knuefermann P, Lakshminarayanan V, Dewald O, Evans AJ, Peschon J, Mann DL, Michael LH, Entman ML (2001) *Am J Physiol Heart Circ Physiol* 281:H2549–H2558.
10. Dewald O, Frangogiannis NG, Zoerlein M, Duerr GD, Klemm C, Knuefermann P, Taffet G, Michael LH, Crapo JD, Welz A, Entman ML (2003) *Proc Natl Acad Sci USA* 100:2700–2705.
11. Dewald O, Frangogiannis NG, Zoerlein MP, Duerr GD, Taffet G, Michael LH, Welz A, Entman ML (2004) *J Thorac Cardiovasc Surg* 52:305–311.
12. Frangogiannis NG, Shimoni S, Chang SM, Ren G, Shan K, Aggeli C, Reardon MJ, Letsou GV, Espada R, Ramchandani M, *et al.* (2002) *Am J Pathol* 160:1425–1433.
13. Frangogiannis NG, Shimoni S, Chang SM, Ren G, Dewald O, Gersch C, Shan K, Aggeli C, Reardon M, Letsou GV, *et al.* (2002) *J Am Coll Cardiol* 39:1468–1474.
14. Dewald O, Ren G, Winkelmann K, Koerting A, Kraemer D, Taffet G, Rollins BJ, Entman ML, Frangogiannis NG (2004) *Circulation* 110(Suppl 17):320–321.
15. Quan TE, Cowper S, Wu SP, Bockenstedt LK, Bucala R (2004) *Int J Biochem Cell Biol* 36:598–606.
16. Metz CN (2003) *Cell Mol Life Sci* 60:1342–1350.
17. Pilling D, Buckley CD, Salmon M, Gomer RH (2003) *J Immunol* 171:5537–5546.
18. Goodell MA, Jackson KA, Majka SM, Mi T, Wang H, Pocius J, Hartley CJ, Majesky MW, Entman ML, Michael LH, Hirschi KK (2001) *Ann NY Acad Sci* 938:208–218.
19. Jackson KA, Majka SM, Wang H, Pocius J, Hartley CJ, Majesky MW, Entman ML, Michael LH, Hirschi KK, Goodell MA (2001) *J Clin Invest* 107:1395–1402.
20. Kucia M, Dawn B, Hunt G, Guo Y, Wysoczynski M, Majka M, Ratajczak J, Rezzoug F, Ildstad ST, Bolli R, Ratajczak MZ (2004) *Circ Res* 95:1191–1199.
21. Vasa M, Fichtlscherer S, Aicher A, Adler K, Urbich C, Martin H, Zeiher AM, Dimmeler S (2001) *Circ Res* 89:E1–E7.
22. Orlic D, Kajstura J, Chimenti S, Jakoniuk I, Anderson SM, Li B, Pickel J, McKay R, Nadal-Ginard B, Bodine DM, *et al.* (2001) *Nature* 410:701–705.
23. Nadal-Ginard B, Kajstura J, Leri A, Anversa P (2003) *Circ Res* 92:139–150.
24. Frangogiannis NG, Perrard JL, Mendoza LH, Burns AR, Lindsey ML, Ballantyne CM, Michael LH, Smith CW, Entman ML (1998) *Circulation* 98:687–698.
25. Hashimoto N, Jin H, Liu T, Chensue SW, Phan SH (2004) *J Clin Invest* 113:243–252.
26. Mori L, Bellini A, Stacey MA, Schmidt M, Mattoli S (2005) *Exp Cell Res* 304:81–90.
27. Lama VN, Phan SH (2006) *Proc Am Thorac Soc* 3:373–376.
28. Abe R, Donnelly SC, Peng T, Bucala R, Metz CN (2001) *J Immunol* 166:7556–7562.
29. Steel DM, Whitehead AS (1994) *Immunol Today* 15:81–88.
30. Mold C, Baca R, Du Clos TW (2002) *J Autoimmun* 19:147–154.
31. Pilling D, Tucker NM, Gomer RH (2006) *J Leukocyte Biol* 79:1242–1251.
32. Daeron M (1997) *Annu Rev Immunol* 15:203–234.
33. Hawkins PN, Tennent GA, Woo P, Pepys MB (1991) *Clin Exp Immunol* 84:308–316.